Deep learning based reduced order modeling of seismogram-type acceleration time series model: Part - I

Saumik Dana[1*] and Karthik Reddy[2]

[1*]University of Southern California, Los Angeles, CA, USA.
[2]North Carolina State University, Raleigh, NC, USA.

*Corresponding author(s). E-mail(s): saumik@utexas.edu;
Contributing authors: klyatha@ncsu.edu;

Abstract

The critical slip distance in rate and state model for fault friction in the study of earthquakes can vary wildly from micrometers to few meters depending on the length scale of the critically stressed fault. This makes it incredibly important to construct a Bayesian inversion framework that provides good estimates of the critical slip distance based on the observed acceleration at the seismogram. That estimate eventually helps in predicting future seismic behavior. To eventually construct such a framework for real data, we first work on synthetic data. This data is generated by adding noise to the acceleration output of spring-slider-damper idealization of the rate and state model as the forward model. Furthermore, the forward model in real-time field studies can be incredibly complicated, and constructing a reduced order model is of paramount importance for the Bayesian framework to be a starter in the first place. With that in mind, we use deep learning architecture of LSTM encoder-decoder towards constructing a reduced order model for the spring-slider-damper idealization. This is part-I in a series of research studies.

Keywords: Fault friction, rate and state model, critical slip distance, LSTM, encoder, decoder

1 Introduction

The acceleration recorded by seismograms on the earth's surface are a manifestation of subsurface activity resulting out of a myriad of energy technologies and climate mitigation goals. While the seismicity can be classified as microseismicity, felt seismicity and major earthquakes, the seismogram continues to record the acceleration time series on a continuous basis. That lends to richness of data which can be used to infer properties of the subsurface for eventual accurate predictions of seismic behavior. There are a lot of properties pertaining to the subsurface like rock moduli and flow permeability, but typically the inference framework makes sense for properties that cannot be estimated with a fair degree of certainty even with substantial domain expertise. The critical slip distance in the fault friction model is one such parameter. To provide some perspective: The quantification of fault slip is achieved using the rate-and state-friction (RSF) model for modeling earthquake cycles on faults [1–6], and given by

$$\begin{gathered}\mu = \mu_0 + A \ln\left(\frac{V}{V_0}\right) + B \ln\left(\frac{V_0\theta}{d_c}\right), \\ \frac{d\theta}{dt} = 1 - \frac{\theta V}{d_c}\end{gathered} \tag{1}$$

where $V = |\frac{d\boldsymbol{d}}{dt}|$ is the slip rate magnitude, $a = \frac{dV}{dt}$ which we hypothesize is of the same order as recorded by seismograph, μ_0 is the steady-state friction coefficient at the reference slip rate V_0, A and B are empirical dimensionless constants, θ is the macroscopic variable characterizing state of the surface and d_c is a critical slip distance over which a fault loses or regains its frictional strength after a perturbation in the loading conditions [7]. Regardless of the importance, it is paradoxical that the values of d_c reported in the literature range from a few to tens of microns to few meters [8–10]. With that in mind, we got to provide a Bayesian inference framework in which synthetic earthquake data is used to estimate critical slip distance. In the Bayesian framework, the forward model is continually evaluated as the inference proceeds, and if the forward model is too complicated as in coupled flow and poromechanics [11–20], it can lead to a total breakdown of the inference framework in terms of feasibility. That is the reason why a reduced order model needs to be generated, which is then used to give quick forward estimations inside the Bayesian loop. While there are mathematical concepts like principal component analysis and proper orthogonal decompositions which are neat in theory, the implementation needs to equally clean, and this is where deep learning is very helpful.

The popular architecture for reduced order modeling of computational physics is Long short term memory (LSTM) [22] Encoder Decoder (LSTM ED), which is basically an encoder network with LSTM cells followed by a decoder with LSTM cells, as shown in Fig. 1. The encoder attempts to compress the temporal information into a vector or a series of vectors which capture as many features as are important, and the decoder decodes that tuple to reconstruct the time series. LSTMs (Fig. 2) have traditionally been used in

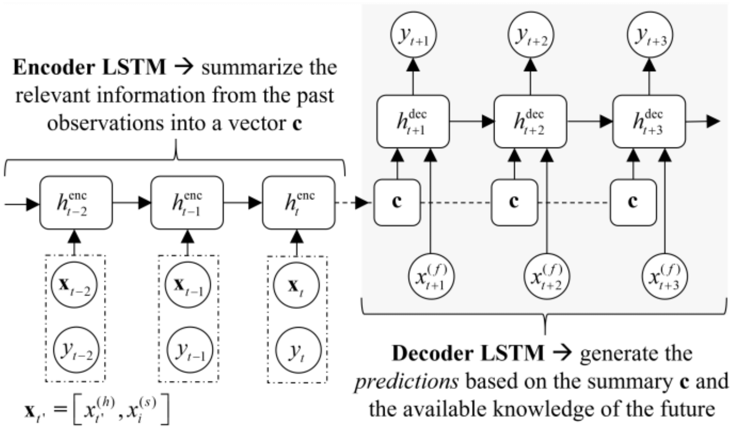

Fig. 1: LSTM encoder decoder (Graphic from [21])

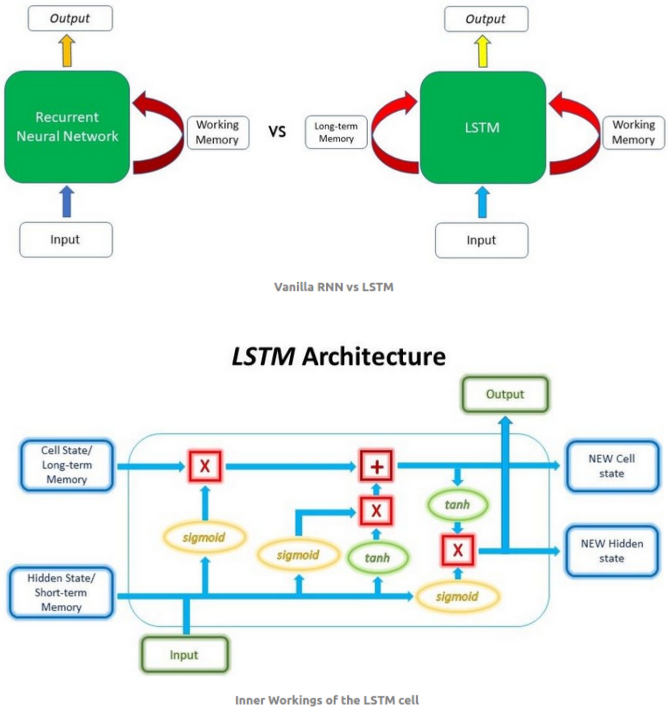

Fig. 2: Long short term memory (LSTM) is geared towards prediction and eventually reconstruction of time series data

natural language processing, although there is a shift towards using the transformers in this realm. The ubiquity of LSTM implementations in PyTorch and

TensorFlow and the correspondence between encoders and the mathematical concept of principal component analysis makes LSTMs still very popular for reconstruction of time series data using a reduced basis set. There are two things here: prediction and reconstruction. Prediction is when a certain piece of the data is used to train the LSTM ED, and then the LSTM ED makes a prediction for the remaining piece of the data. On the other hand, reconstruction is when the entire data set is fed into the encoder, which then encodes the information and feeds it to the decoder for reconstruction, thereby lending a reduced order model. The latter is harder than the former, and we start with building a framework for prediction before moving onto reconstruction.

1.1 The forward model

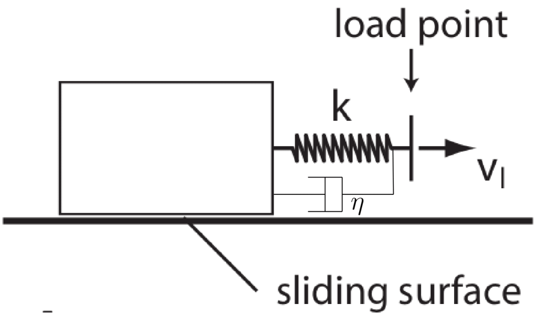

Fig. 3: Spring slider damper idealization of fault behavior

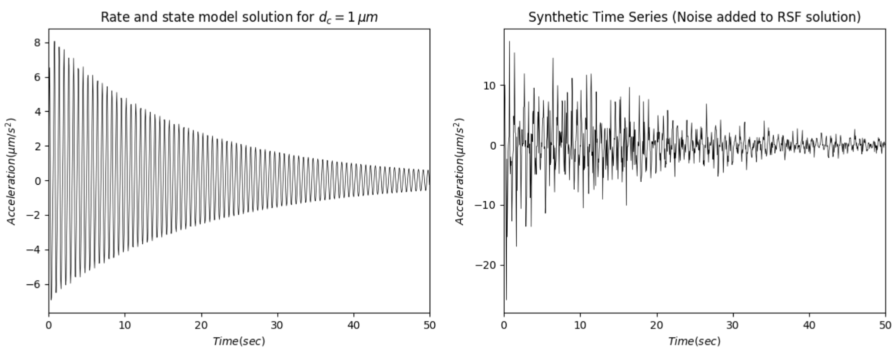

Fig. 4: System response

As shown in Fig. 3, we model a fault by a slider spring system [23–25]. The influence of critical slip distance on system response to a load point perturbation of the form

$$V_l = V_0(1 + \exp{(-t/20)}\, sin(10t)) \tag{2}$$

is shown in Fig. 4. The details of the forward model are given in Appendix A.

2 LSTM encoder-decoder results

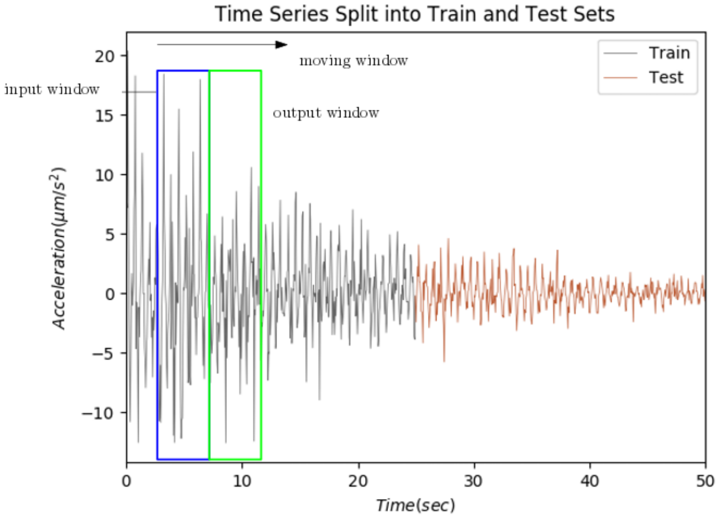

Fig. 5: Data is processed in moving windows for the LSTM encoder decoder framework. The distance between the moving windows is called stride. In our study, we fix the output window and stride, and vary the input window to check the efficacy of the LSTM encoder decoder framework in making time series predictions

The time series data is first split into training and test data, and then the LSTM ED works on chunks of data within the training and test data sets respectively. This chunk of data is called a window, and within window there is an input window used to train the LSTM ED, and an output window used to test the LSTM ED. This window traverses through the training and test data sets in strides, as shown in Fig. 5. As shown in Figs. 6- 8, the performance gets better if the input window is increased. The code was implemented in PyTorch, and run on a very basic AMD Ryzen 3 3200U with Radeon Vega Mobile Gfx $\times$ 4 processor

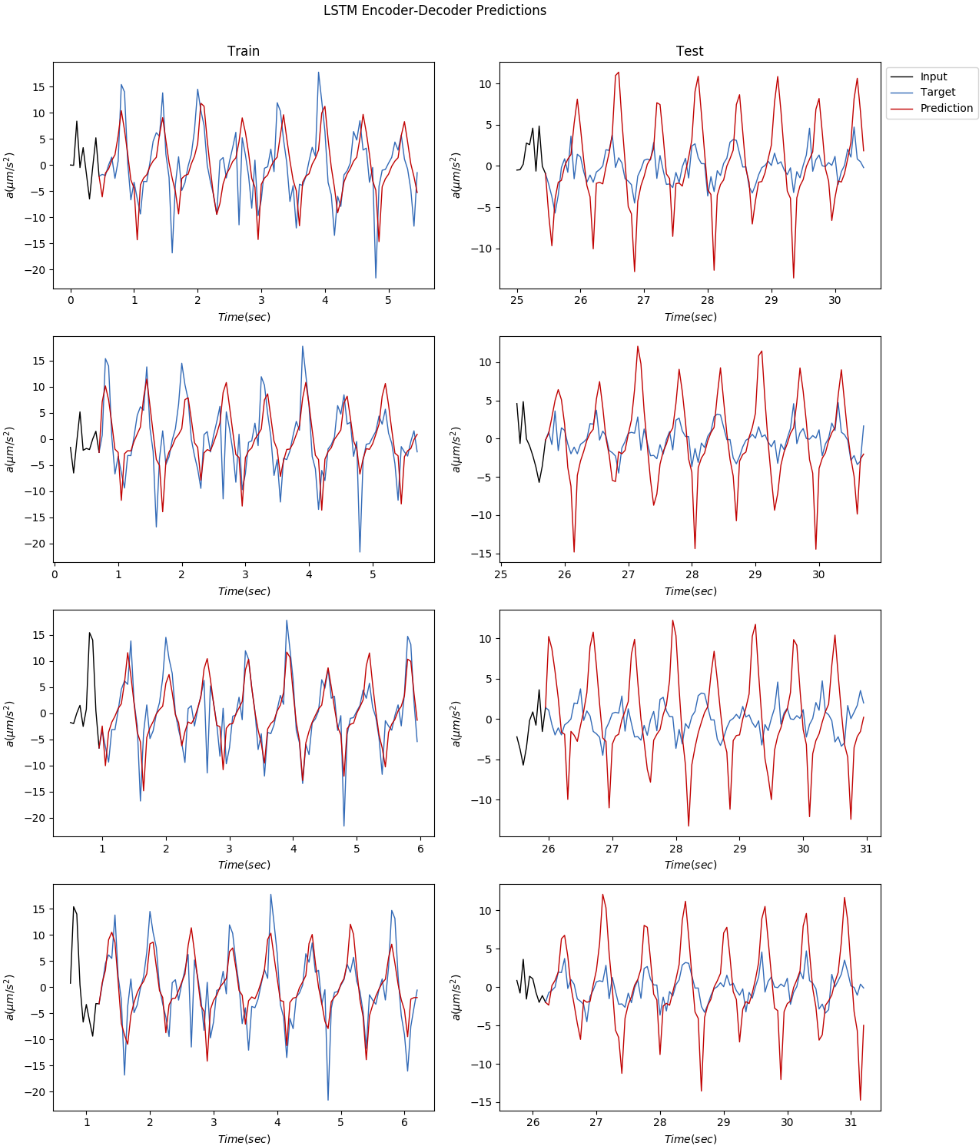

Fig. 6: Predictions are made in the output window of size 100 for the model trained in the input window of size 10 for the first 4 moving windows of both train and test data sets

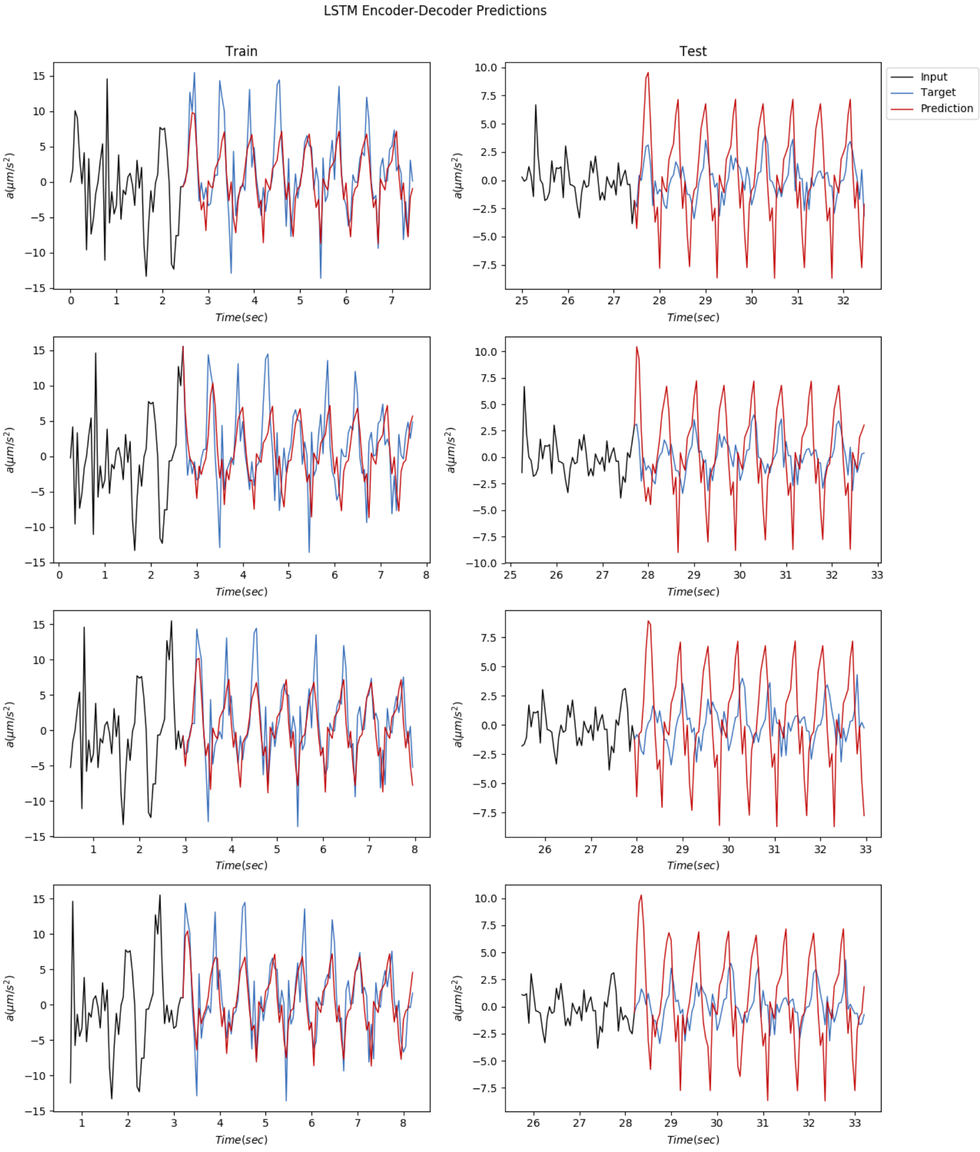

Fig. 7: Predictions are made in the output window of size 100 for the model trained in the input window of size 50 for the first 4 moving windows of both train and test data sets

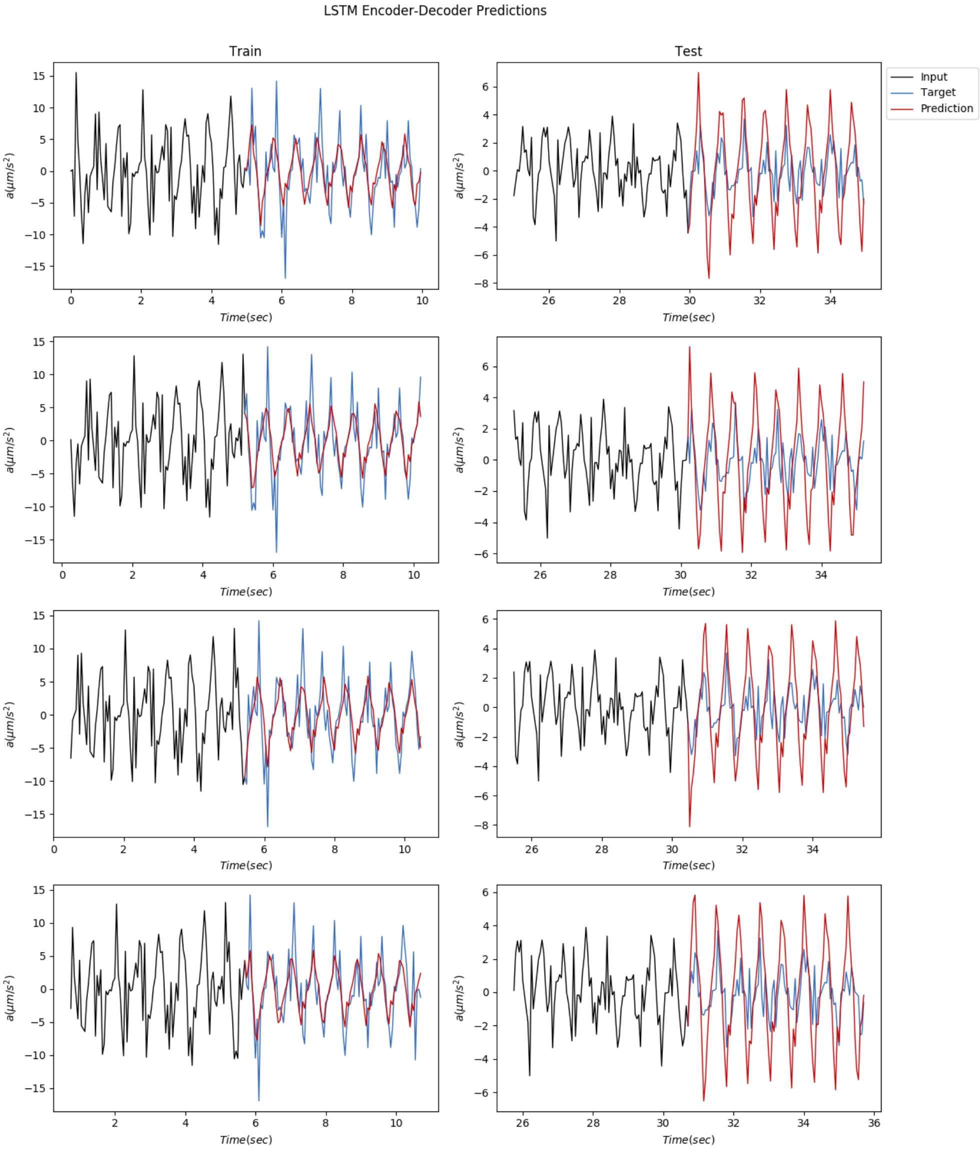

Fig. 8: Predictions are made in the output window of size 100 for the model trained in the input window of size 100 for the first 4 moving windows of both train and test data sets

Appendix A Forward model details

The friction coefficient of the block is given by

$$\mu = \frac{\tau}{\sigma} = \frac{\tau_l - k\delta - \eta V}{\sigma} \tag{A1}$$

where σ is the normal stress, τ the shear stress on the interface, τ_l is the remotely applied stress acting on the fault in the absence of slip, -$k\delta$ is the decrease in stress due to fault slip [26] and η is the radiation damping coefficient [27]. We consider the case of a constant stressing rate $\dot{\tau}_l = kV_l$ where V_l is the load point velocity. The initial stress may be smaller or larger than steady state friction owing to coseismic slip on the fault patch or on adjacent parts of the fault. The expression neglects inertia, and is thus only valid for low slip speed in the interseismic period. The stiffness is a function of the fault length l and elastic modulus E as $k \approx \frac{E}{l}$. With $k' = \frac{E}{l\sigma}$, we get

$$\dot{\mu} \approx k'(V_l - V) - k''\dot{V} \tag{A2}$$

where $k'' = \frac{\eta}{\sigma}$. Once the phenomenological form of $\dot{\mu}$ is known, we rewrite Eq. (1) as

$$\begin{gathered} V = V_0 \exp\left(\tfrac{1}{A}\left(\mu - \mu_0 - B\ln\left(\tfrac{V_0\theta}{d_c}\right)\right)\right), \\ \dot{\theta} = 1 - \tfrac{\theta V}{d_c} \end{gathered} \tag{A3}$$

to get acceleration time series as $a \equiv \dot{V}$ as,

$$\begin{aligned} \dot{V} &= \frac{V}{A}\left(\dot{\mu} - \frac{B}{\theta}\dot{\theta}\right) \\ &= \frac{V_0 \exp\left(\frac{1}{A}\left(\mu - \mu_0 - B\ln\left(\frac{V_0\theta}{d_c}\right)\right)\right)}{A} \\ &\quad * \left(k'\left(V_l - V_0\exp\left(\frac{1}{A}\left(\mu - \mu_0 - B\ln\left(\frac{V_0\theta}{d_c}\right)\right)\right)\right) - k''\dot{V} - \frac{B}{\theta}\left(1 - \frac{\theta V}{d_c}\right)\right) \end{aligned} \tag{A4}$$

The ballpark values are:

✓ Elastic modulus $E = 5 \times 10^{10}\, Pa$
✓ Critical fault length $l = 3 \times 10^{-2}\, m$
✓ Normal stress $\sigma = 200 \times 10^6 Pa$
✓ Radiation damping coefficient $\eta = 20 \times 10^6 Pa/(m/s)$
✓ $A = 0.011$
✓ $B = 0.014$
✓ $V_0 = 1\mu m/s$
✓ $\theta_0 = 0.6$
✓ $\mu_0 = \mu_0 = 0.6$
✓ $t_{start} = 0$, $t_{end} = 50\, s$, $dt = 0.05\, s$

from which the effective stiffness and damping are obtained as

✓ $k' = \frac{E}{l\sigma} = \frac{5\times10^{10}}{3\times10^{-2}\times2\times10^{8}}[1/m] \approx 10^{-2}[1/\mu m]$

✓ $k'' = \frac{\eta}{\sigma} = \frac{2\times10^{7}}{2\times10^{8}}[s/m] = 10^{-7}[s/\mu m]$

References

[1] Ruina, A.L.: Slip instability and state variable friction laws. Geophys. Res. Lett. **88**, 359–370 (1983)

[2] Scholz, C.H.: Mechanics of faulting. Ann. Rev. Earth Planet. Sci. **17**, 309–334 (1989)

[3] Marone, C.: Laboratory-derived friction laws and their application to seismic faulting. Ann. Rev. Earth Planet. Sci. **26**, 643–696 (1998)

[4] Wei, M., Shi, P.: Synchronization of earthquake cycles of adjacent segments on oceanic transform faults revealed by numerical simulation in the framework of rate-and-state friction. Journal of Geophysical Research: Solid Earth **126**(1), 2020–020231 (2021)

[5] Jia, Y., Tang, J., Lu, Y., Lu, Z.: The effect of fluid pressure on frictional stability transition from velocity strengthening to velocity weakening and critical slip distance evolution in shale reservoirs. Geomechanics and Geophysics for Geo-Energy and Geo-Resources **7**(1), 1–13 (2021)

[6] Weiqiang, Z., Allison, K., Dunham, E., Yang, Y.: Fault valving and pore pressure evolution in simulations of earthquake sequences and aseismic slip. Nature communications **11**, 4833 (2020)

[7] Palmer, A.C., Rice, J.R.: The growth of slip surfaces in the progressive failure of over-consolidated clay. Proceedings of the Royal Society of London. A. Mathematical and Physical Sciences **332**(1591), 527–548 (1973)

[8] Kaneko, Y., Fukuyama, E., Hamling, I.J.: Slip-weakening distance and energy budget inferred from near-fault ground deformation during the 2016 mw7. 8 kaikōura earthquake. Geophysical Research Letters **44**(10), 4765–4773 (2017)

[9] Niemeijer, A., Di Toro, G., Nielsen, S., Di Felice, F.: Frictional melting of gabbro under extreme experimental conditions of normal stress, acceleration, and sliding velocity. Journal of Geophysical Research: Solid Earth **116**(B7) (2011)

[10] Ohnaka, M.: A constitutive scaling law and a unified comprehension for frictional slip failure, shear fracture of intact rock, and earthquake rupture. Journal of Geophysical Research: Solid Earth **108**(B2) (2003)

[11] Dana, S., Lyathakula, K.R.: Uncertainty quantification in friction model for earthquakes using bayesian inference. arXiv preprint arXiv:2104.11156 (2021)

[12] Dana, S., Wheeler, M.F.: Convergence analysis of fixed stress split iterative scheme for anisotropic poroelasticity with tensor biot parameter. Computational Geosciences **22**(5), 1219–1230 (2018)

[13] Dana, S., Wheeler, M.F.: Convergence analysis of two-grid fixed stress split iterative scheme for coupled flow and deformation in heterogeneous poroelastic media. Computer Methods in Applied Mechanics and Engineering **341**, 788–806 (2018)

[14] Dana, S., Wheeler, M.F.: Design of convergence criterion for fixed stress split iterative scheme for small strain anisotropic poroelastoplasticity coupled with single phase flow. arXiv preprint arXiv:1912.06476 (2019)

[15] Dana, S., Ganis, B., Wheeler, M.F.: A multiscale fixed stress split iterative scheme for coupled flow and poromechanics in deep subsurface reservoirs. Journal of Computational Physics **352**, 1–22 (2018)

[16] Dana, S., Jammoul, M., Wheeler, M.F.: Performance studies of the fixed stress split algorithm for immiscible two-phase flow coupled with linear poromechanics. Computational Geosciences, 1–15 (2021)

[17] Dana, S., Srinivasan, S., Karra, S., Makedonska, N., Hyman, J.D., O'Malley, D., Viswanathan, H., Srinivasan, G.: Towards real-time forecasting of natural gas production by harnessing graph theory for stochastic discrete fracture networks. Journal of Petroleum Science and Engineering **195**, 107791 (2020)

[18] Dana, S., Ita, J., Wheeler, M.F.: The correspondence between voigt and reuss bounds and the decoupling constraint in a two-grid staggered algorithm for consolidation in heterogeneous porous media. Multiscale Modeling & Simulation **18**(1), 221–239 (2020)

[19] Dana, S.: Addressing challenges in modeling of coupled flow and poromechanics in deep subsurface reservoirs. PhD thesis, The University of Texas at Austin (2018)

[20] Dana, S., Reddy, K.: Bayesian inference and markov chain monte carlo based estimation of a geoscience model parameter. arXiv preprint arXiv:2201.01868 (2021)

[21] Bottieau, J., Hubert, L., De Grève, Z., Vallée, F., Toubeau, J.-F.: Very-short-term probabilistic forecasting for a risk-aware participation in the single price imbalance settlement. IEEE Transactions on Power Systems

35(2), 1218–1230 (2019)

[22] Sak, H., Senior, A., Beaufays, F.: Long short-term memory based recurrent neural network architectures for large vocabulary speech recognition. arXiv preprint arXiv:1402.1128 (2014)

[23] Rice, J.R., Gu, J.-c.: Earthquake aftereffects and triggered seismic phenomena. Pure and Applied Geophysics **121**(2), 187–219 (1983)

[24] Gu, J.-C., Rice, J.R., Ruina, A.L., Simon, T.T.: Slip motion and stability of a single degree of freedom elastic system with rate and state dependent friction. Journal of the Mechanics and Physics of Solids **32**(3), 167–196 (1984)

[25] Dieterich, J.H.: Earthquake nucleation on faults with rate-and state-dependent strength. Tectonophysics **211**(1-4), 115–134 (1992)

[26] Kanamori, H., Brodsky, E.E.: The physics of earthquakes. Reports on Progress in Physics **67**(8), 1429 (2004)

[27] McClure, M.W., Horne, R.N.: Investigation of injection-induced seismicity using a coupled fluid flow and rate/state friction model. Geophysics **76**(6), 181–198 (2011)